Journal of Applied Polymer Science

Innovative Direct Nanoparticle Dispersion Injection into Injection Molding Processing

Irene Hassinger,[1] Thorsten Becker,[1] Rolf Walter,[1] Thomas Burkhart,[1] Michael Kopnarski,[2] Alexander Brodyanski[2]

[1]Institute for Composite Materials, Technical University of Kaiserslautern, Erwin-Schrödinger-Str. D-67663 Kaiserslautern, Germany

[2]Institute for Surface and Thin Film Analytics, IFOS GmbH, Trippstadter Strasse 120, D-67663 Kaiserslautern, Germany

Correspondence to: I. Hassinger (E-mail: irene.hassinger@ivw.uni-kl.de)

ABSTRACT: Nanoparticles are applied in polymer matrices because of building up an inorganic network within an organic network resulting in a simultaneous increase of stiffness and toughness provided that a good degree of dispersion with a very low amount of agglomerates can be realized. To prevent these kinds of agglomerates, the incorporation of appropriate nanoparticle dispersions is promising. Using nanoparticle containing dispersions, we can produce nanocomposites via a direct injection molding process with excellent nanoparticle dispersion in the resulting nanocomposite. TiO_2- (15 nm and 300 nm) and Al_2O_3- (13 nm) particle containing dispersions were manufactured and incorporated in polyamide 6 (PA6) via the addition of a nanoparticle containing dispersion within an injection molding process (IM). Agglomeration has to be suppressed during injection molding process and the nanoparticles have to cross over from the dispersing agent to the polymer matrix melt in which they have to be well distributed. The resulting mechanical (tensile and Charpy impact) and morphological (SEM and TEM) properties of those nanocomposites are discussed. The impact toughness and Young's modulus could be enhanced with slightly decreasing tensile strength. The nanoparticles could be well distributed in the polymer matrix. The achievable distribution quality is equal to the distribution achieved in a melt kneading process. Thus, materials with enhanced elongation at break with a very good dispersion quality were produced in a single production process. © 2014 Wiley Periodicals, Inc. J. Appl. Polym. Sci. **2014**, *131*, 40641.

KEYWORDS: extrusion; mechanical properties; morphology; nanostructured polymers; polyamides

Received 18 October 2013; accepted 23 February 2014

DOI: 10.1002/app.40641

INTRODUCTION

Protective equipments, like ballistic protective helmets, need high stiffness and high impact toughness. The stiffness, impact toughness and tensile strength of nanoparticle-filled polymers can be increased simultaneously.[1] Nanoparticles impact on mechanical properties depends on their dimensions, e.g., decreasing particle radius increases specific surface area in a reciprocal way. Thus, nanoparticles play a very important role in polymers due to their high specific surface area,[2] but they also built up agglomerates due to van der Waal's forces in order to reduce their surface activity.[3] These agglomerates behave like microparticles reinforcement of thermoplastic polymers increasing stiffness but decreasing impact toughness and tensile strength.[4,5]

Many processes exist to produce particle-reinforced thermoplastics, the economically most important of which is the continuous extrusion process.[6] Research has shown that shear energy input during extrusion processes is not sufficient to break up all existing agglomerates, not even when multiple extrusion is applied.[7,8] In this method a masterbatch is produced and extruded several times to deagglomerate the nanoparticles and disperse them in the matrix. To improve the economic viability of this approach, the number of process steps has to be reduced. The most interesting process is one that would produce nanocomposites in one step. The goal of this work is, therefore, the manufacture of nanoparticle-modified polymeric parts in a single injection molding (IM) shot without premixing or compounding.

The shear energy input in an injection molding machine is even less than that within a twin screw extruder by what deagglomeration does not take place in injection molding. To produce nanocomposites using IM one needs to apply nanoparticles containing dispersions. In IM just using water as a dispersing agent is not the right path forward, as evaporation of water vapor is impossible in IM. In our case we used a polysorbate as a dispersing agent to produce nanoparticle-containing dispersions without the need for an evaporation process. The polysorbate

Table I. List of Produced Compounds (Only Containing A Priori Dispersed Tween-nanoparticle Dispersions) via Injection Molding and Kneader. (*ml of the Tween-nanoparticle Dispersion Used in Each Injection Cycle)

Particle	Product name	Production method	Dispersion concentration (wt %)	mL dispersion per injection *	Final filler concentration in polymer (vol %)
		Injection molding	0	1	0
TiO_2	Kronos	Injection molding	50	1	0.5
TiO_2	Kronos	Injection molding	71.8	1	1.0, 1.4, 2.1
TiO_2	RM300	Injection molding	42.9	1	0.6, 1.2
Al_2O_3	AluC	Injection molding	24.1	3	0.2, 0.4
TiO_2	Kronos	Kneader	71.8	2.4	2.3
TiO_2	RM300	Kneader	42.9	6.3	2.1
Al_2O_3	AluC	Kneader	24.1	12.5	1.6

can stay within PA 6, acting like a plasticizer. Tween 20 is the selected polysorbate and has a thermal stability of over 250°C.

The company NOVOSYSTEMS Farben & Additive GmbH successfully produces color liquids (pigment dispersions) for IM processes by using different carrier materials (dependent on the polymer and color) and additives (UV-stabilizers, defoaming agents) in what case dispersing agents remain in the matrix. Within the project NanoDirekt[9] it was found that nanoparticles can be incorporated into polymer matrices via twin screw extrusion by adding nanoparticle-water suspension [carbon nanotubes (CNT), Aerosil, MMT] with subsequent degassing process steps. The resulting materials showed a good dispersion quality and good mechanical properties. The manufacturing of noncontinuous products (e.g., profiles) requires a further processing step such as thermoforming or injection molding. Frache et al.[10] showed that nanocomposites can also be prepared via direct-injection molding using mixtures based on polymer and particle powders. The resulting dispersion qualities are comparable to those of twin screw extruded nanocomposites.

EXPERIMENTAL

Material

In the case of PA6 we used Ultramid B 24 N 03 (BASF SE, Germany), a commercially available light stabilized polyamide 6 grade which is especially suitable for high speed spinning to produce textile fibres. Three nanofillers were applied. First, a commercially available titanium dioxide particle powder (HOMBITEC RM 300, Sachtleben Chemie GmbH, Germany) with an average primary particle size of 15 nm and an average specific surface area of 70 m^2/g was used (here labelled "RM300") (in accordance with the manufacturer's data). The particle surface was functionalized with polyalcohol by the producer. Second, a commercially available titanium dioxide (TiO_2) particle powder (Kronos 2310, KRONOS Worldwide, Inc., Germany, USA) with a nominal average primary particle size of 300 nm was selected (here labelled "Kronos"). The latter particles were inorganically treated with aluminum, silicon and zirconium. We chose a TiO_2-particel because of convincing results in PA 6.6 due to a very good particle-matrix interphase.[7] The third nanofiller was a commercially available aluminum oxide (Al_2O_3) (AEROXIDE® Alu C, Evonik Industries AG, Germany) with a nominal average primary particle size of 13 nm and a specific surface area of 100 m^2/g. Al_2O_3 was chosen because of its very good dispersability (here labelled "AluC"). As dispersing agent the polysorbate Tween® 20 (Polyoxyethylen-20-sorbitanmonolaurat, Carl Roth GmbH + Co. KG, Germany) was used, with a decomposition temperature higher than 250°C (here labeled "Tween").

Production of Dispersions

The nanoparticles were dispersed in a top-down process using polysorbate 20 (Tween® 20) as a dispersing agent. The TiO_2 nanoparticles (Kronos, according to manufacturer 300 nm in diameter) were dispersed using a dissolver (AE01-10Mm, VMA Getzmann GmbH, Germany) at a rotation speed of 5800 min^{-1} under vacuum for 15 min. Two dispersions containing 50 wt % and 71.8 wt % of TiO_2 were produced. The TiO_2 (RM300) with a nominal diameter of 15 nm and the Al_2O_3 (AluC) with a nominal diameter of 13 nm were dissolved in Tween® 20 in a pearl mill (SL 12 C1, VMA Getzmann GmbH, Germany). The dispersions were milled for 45 min at 3000 rpm at 53°C. The TiO_2-(RM300)-Tween dispersion contains 42.9 wt % of TiO_2, the Al_2O_3-(AluC)-Tween dispersion contains 24.1 wt % of Al_2O_3.

Injection Molding

Before running injection molding, PA 6 was dried for 24 h at 80°C. Test specimens for impact and tensile testing were prepared using an injection molding machine (Allrounder 320, Arburg GmbH, Germany). The nanoparticle-containing dispersions were directly, manually injected into the hopper of the injection molding machine at the same time as the PA6 granules.

Material Production with Measuring Kneader

Before compounding, PA 6 was dried for 24 h at 80°C. Kneading was carried out with a measuring kneader (Brabender, Brabender GmbH, Germany) at 250°C and 100 rpm for 8 min.

List of Materials

Table I gives an overview of the materials produced via injection molding and kneading.

Charpy

Before mechanical testing the specimens were dried at 80°C for 3 days.

The Charpy impact toughness was measured according to DIN EN ISO 179 on a pendulum-type impact testing machine

(CEAST GmbH, Germany). The specimens were of Type 1 with a notch of Type A. The bearing distance was set to 62 mm with an impact energy of 4 J and an impact speed of 2.9 m/s.

Tensile Tests

Before mechanical testing the specimens were dried at 80°C for 3 days.

Tensile tests were performed at room temperature on injection-molded specimens in accordance to DIN EN ISO 527-2 standard on a universal testing machine (Zwick GmbH model 1485, Germany). The specimens were of Type 1A measured with 2 mm/min.

Scanning Electron Microscopy

Polished surfaces were analyzed using an electron microscope (Supra 40, Carl Zeiss AG, Germany) via detecting the backscattering electrons. Fracture surfaces were scanned using a secondary electron detector. Before all samples were coated with gold using a Sputtering Device (SCD – 050, Balzer AG, Switzerland).

Transmission Electron Microscopy

The TEM-examination of the samples was carried out using a Jeol 2010 transmission electron microscope (thermionic LaB_6 cathode, Jeol, Japan) equipped with an electron energy imaging filter GIF Tridiem 863 (Gatan, USA). The TEM images were taken at the primary electron energy of 197 keV in an energy filtered mode (EFTEM) using the elastic scattered electrons only (zero-loss images). Energy slit of the energy filter was kept at 10 eV during all acquisitions, whereas the collection angle was varied. The overview images were taken in the LowMag operating mode of the TEM without any objective aperture. The LowMag images reveal the general distribution of the nanoparticles within the polymers. To visualize details of shape and size of single particles and the clusters of particles as well the higher magnifications in the Mag mode of the microscope are required. We used a collection semiangle of about 4.7 mrad to maximize an image contrast at these measurements. The convergency semiangle of the primary electron beam on the sample was 0.42 mrad in the Mag mode and substantially smaller ($\leq$0.1 mrad) during overview imaging.

To avoid degradation of the polymer under an intensive electron beam and to minimize sample contamination during the TEM observations one should keep the fluences as low as possible. On the other side high quality images require good illuminations as well as sufficient exposure time. We found that electron doses of about 10 C/cm^2 are a reasonable compromise in our case. Under these conditions the microscopic images do not indicate any alteration or contamination of the material after electron irradiation.

The thin sections for the TEM investigations were prepared by ultramicrotome cutting using an Ultramicrotome MT-X (Boeckeler Instruments, USA) equipped with diamond knifes (Diatome Switzerland). Because of the ductile character of the composite materials direct cutting could not produce slices of 50–60 nm thickness as we routinely achieved in the cases of conventionally used epoxy resin (e.g., Epofix, Struers Netherland). Since the reached minimum of thickness of 200 nm is not appropriate for the investigations of small nanoparticles by TEM a special preparation procedure was elaborated.

As a prestage 3–5 μm-thick semithin sections were prepared and these were embedded into the standard epoxy resin. Then we cut ultra-thin sections from these epoxy-polymer-epoxy blocks. We used the 6 mm Histo and 3 mm Ultra (35°) diamond knifes to cut semi- and ultra thin sections respectively. Controlled via the interference color of the floating cuts [a] thin sections with a thickness of ~90 nm came to hand in this way. The thickness of the composite polymer regions as obtained by electron energy loss spectroscopy (TEM-EELS) ranged from 80 to 120 nm. Local thickness variations are caused by weak winkling of the polymers during sectioning due to different mechanical properties of the polymer and the epoxy matrix.

RESULTS AND DISCUSSION

Direct Injection Molding of PA6 with Nanoparticle Containing Dispersions Having Tween 20 as Dispersing Agent

The particle contents of such produced reinforced PA6 nanocomposites are listed in Table I. The TiO_2-nanoparticle dispersions can be incorporated very well in contrary to Al_2O_3 which is a question of particle content. In case of Al_2O_3 the dispersion was not completely picked up by the PA6-granules, but partly stayed at the cylinder wall of the injection molding machine.

Nominal 300 nm TiO_2 particles (Kronos) are dispersed very homogeneously in the PA6 matrix via this innovative processing (Figure 1). This method enables the insertion of particles in the matrix without creation of agglomerates bigger than 250 nm. PA6 nanocomposites containing nano-TiO_2 (RM300, nominal 15 nm primary particle size) and nano-Al_2O_3 (AluC) turned out to be dispersed in such a perfect way that the particles cannot be found via SEM on polished surfaces. Figure 2 and 3 reveal a very good distribution of the respective nanoparticles incorporated in PA6 [Figure 2: Nano-TiO_2 (nominal 15 nm); and Figure 3: Nano-Al_2O_3].

The titan dioxide nanoparticles exhibit a rice-grain shape being characteristic of the rutile phase. This can be concluded from our previous TEM studies comparing different crystallographic

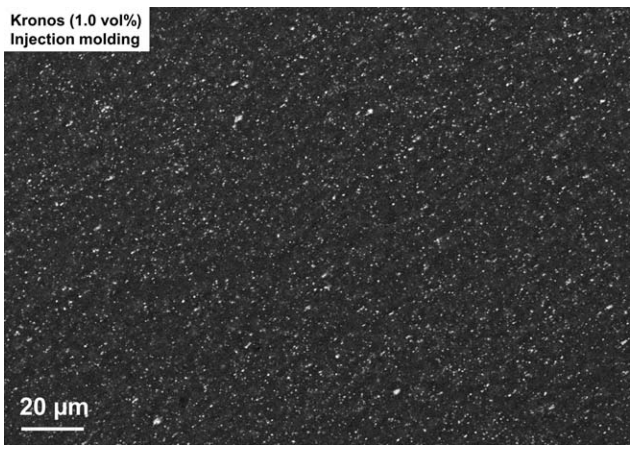

Figure 1. SEM image of TiO_2 sub-microparticles (Kronos) dispersed in a PA6 matrix produced via direct injection molding.

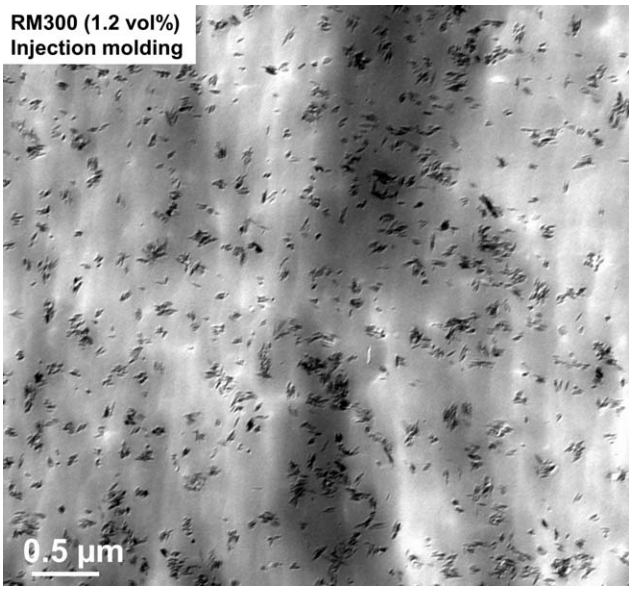

Figure 2. TEM image of TiO_2 nanoparticles (RM300) dispersed in a PA6 matrix produced via direct injection molding.

modifications of TiO_2. The short axis of the particle pattern is of about 10–14 nm whereas in the long direction the length varies within wide limits from 30 to 120 nm.

Both the shape and the size of the alumina nanoparticles differ significantly from the titan dioxide nanoparticles. The Al-oxide nanoparticles have a slightly facetted pebble-like shape with diameters of about 8–12 nm. Sporadic large particles with the sizes up to 19 nm are observed.

All nanocomposites can be produced by a one-step production with a very good dispersion quality. The nanoparticles of both materials are located within the PA6 polymer as small agglomerations. As a rule the agglomerations consist of 2–20 or 5–40

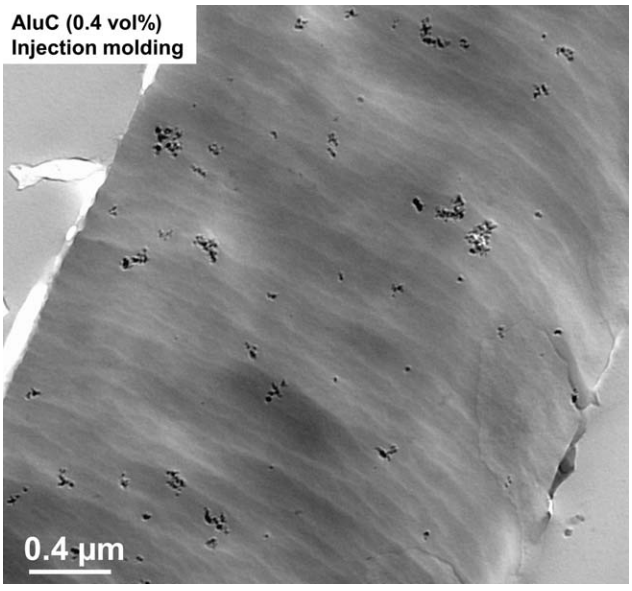

Figure 3. TEM image of Al_2O_3 nanoparticles (AluC) dispersed in a PA6 matrix produced via direct injection molding.

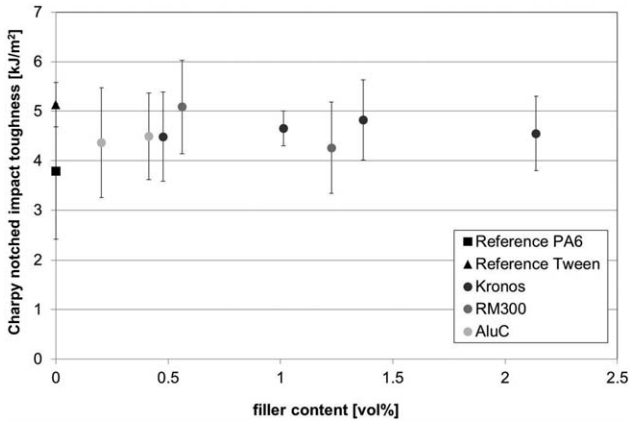

Figure 4. Charpy impact energy as a function of filler concentration for PA6-nanocomposites produced via direct injection molding.

individual nanoparticles in the cases of the rutile and alumina, respectively. Individual particles are very rare in occurrence. This holds for all composite polymers investigated in this work.

From the inspection of our TEM images we cannot solely deduce an influence of the preparation method or the filler concentration on the degree of agglomeration.

The Charpy notched impact toughness (Figure 4) versus the particle filler content reveals that already the dispersing agent Tween 20 increases the impact toughness. In case of Kronos 300 nm TiO_2 particles impact toughness runs through a maximum at around 1.4 vol % particle content. This maximum impact toughness of 4.8 J/m^2 is less than that one using just Tween (impact toughness of 5.1 J/m^2). The maximum impact toughness for nano-TiO_2 (RM300) filled PA6 was detected at 0.6 vol %. This is the same value than neat PA6/Tween and much higher than neat PA6. Al_2O_3 could not be incorporated very well in the matrix because of the insufficient behavior of feeding. Nevertheless, we see an increased impact toughness—at low particle contents (<0.4 vol %)—compared with neat PA6 and an impact toughness compared with that one of Kronos TiO_2

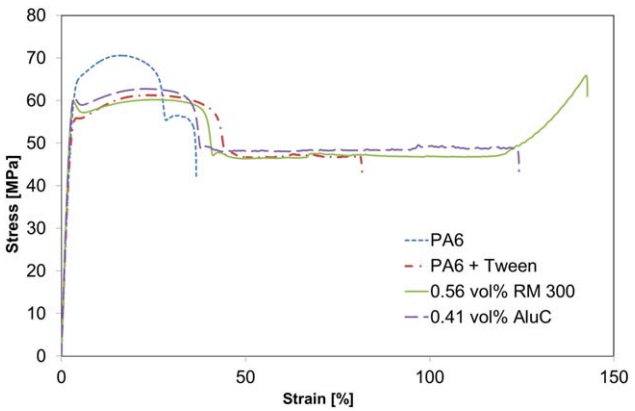

Figure 5. Representative stress-strain diagrams of the tensile tests with the high elongation at break of AluC and RM300 filled nanocomposites clearly visible. With AluC there is a further strain hardening of the materials at high elongations (>120%). [Color figure can be viewed in the online issue, which is available at wileyonlinelibrary.com.]

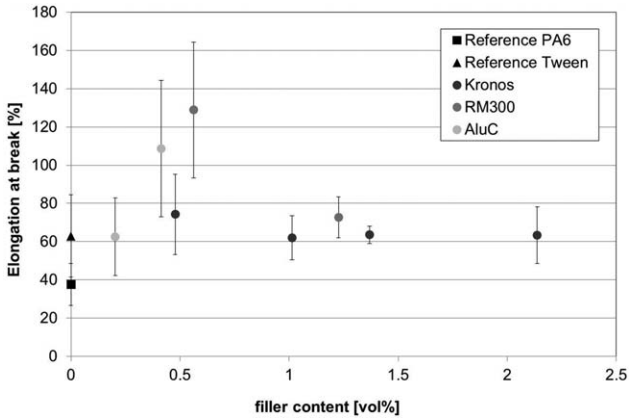

Figure 6. Elongation at break as a function of filler kind and concentration for nanocomposites produced via direct injection molding.

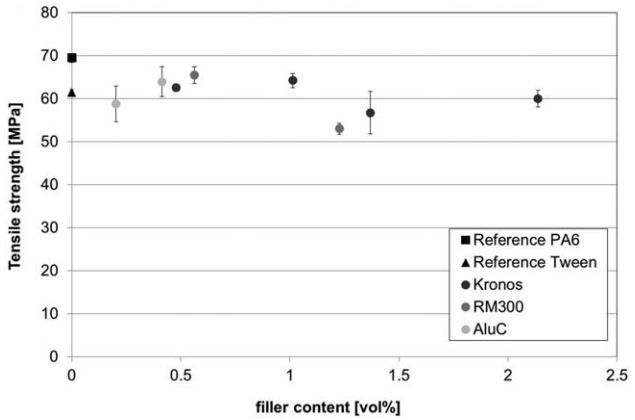

Figure 8. Tensile strength as a function of filler kind and concentration for nanocomposites produced via direct injection molding.

particles with a similar particle content. All particles only marginally increase the impact toughness compared with neat PA6 matrix. Bartczak et al.[1] describe the increase of impact toughness when the interparticle ligament thickness goes below a typical value. For PA6 this critical value is 300 nm.[1] But this applies only for very well dispersed nanoparticles, whereas agglomeration prohibits this increase in impact toughness.[12] In the here presented results, the very small agglomerates prevent the increase of impact toughness in the typical range of 370%.[11]

Figure 5 shows representative stress–strain curves from tensile tests. A high elongation to break of RM300 and AluC-filled nanocomposites is clearly visible. The AluC-filled samples show even a further strengthening of the material at high elongations (>120%).

Figures 6–8 give the respective tensile test results. Figure 6 represents the elongation at break for the respective direct injection molded materials. Blending PA6 with neat Tween increases the elongation at break. The reinforced materials show the same level than Tween-filled material except the 0.41 vol % AluC and 0.56 vol % RM300 filled material. These two materials elongate by factor three higher till they break. The material is very ductile, which is potentially a consequence of the very good particle distribution and the respective particle-matrix interaction. Zhou et al.[13] also found a maximum of elongation at break for SiO_2-reinforced PP at 2 vol % filler content due to a plasticizer effect by the nanoparticles.

Figure 7 reveals a strong increase in E-modulus via Tween 20 incorporation but the rigid metal oxide particles increase the E-modulus even more. The structure of the matrix changes in the interphase region around the nanoparticles. This leads to a property change through nanoparticles. The Young's modulus does not increase linearly with increasing filler content but an increase of about 16% is reached for low filler contents (0.5 vol %) for all kinds of particles (AluC, RM300, and Kronos). For higher filler contents the E-modulus maintains stable on a high level. This is a very interesting result, as usually an increase of Elastic Modulus with increasing volume fraction is found.[14] Our results show, that the mechanical properties are a result of an interplay between nanoparticle-matrix-interaction, particle size, particle size distribution, and dispersion quality. A very flexible interphase can reduce the stiffness by masking the stiffness of the filler.[15,16] Thus, the not occurring increase in stiffness indicates an increased flexibility of the particle-matrix-interphase with increasing volume content. Using IM, 0.5 vol % filler content is sufficient to get a higher stiffness independent

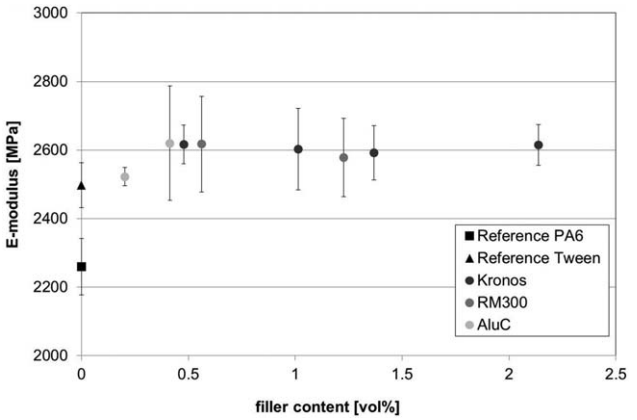

Figure 7. Young's modulus as a function of filler kind and concentration for nanocomposites produced via direct injection molding.

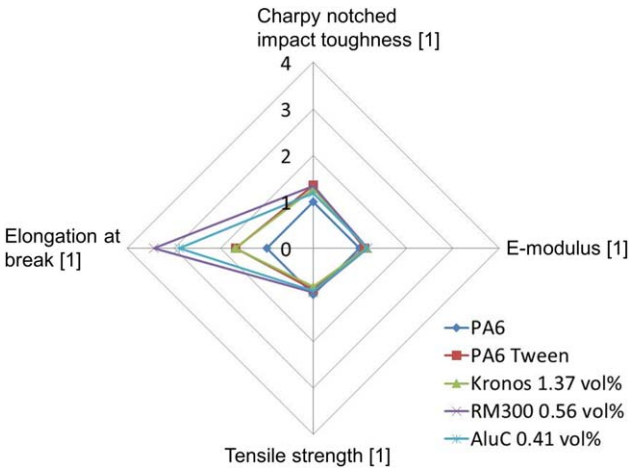

Figure 9. Summary of the mechanical properties of three selected particle reinforced nano- and sub-microcomposites. [Color figure can be viewed in the online issue, which is available at wileyonlinelibrary.com.]

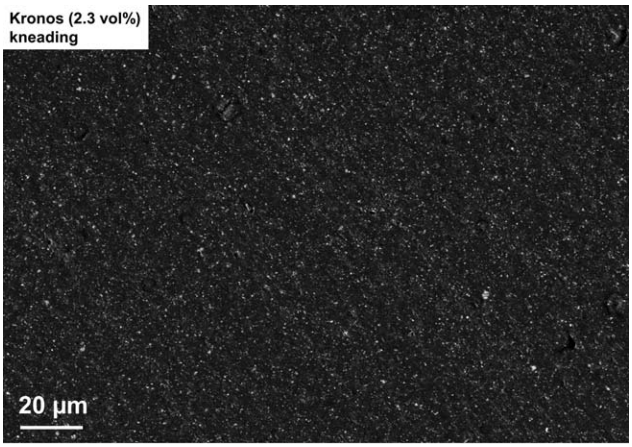

Figure 10. REM image of the polished surface of a compound of PA6 as matrix and the TiO_2 sub-microparticles (Kronos) produced via kneading.

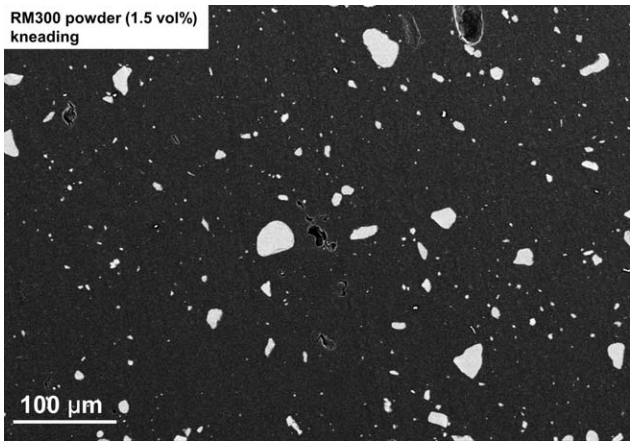

Figure 12. REM image of RM300 TiO_2 nanoparticle powder incorporated in the PA6 matrix in a kneader.

of the used particle. Even for the 300 nm TiO_2 particles (Kronos) the particle surface area seems to be large enough to reach a maximum in E-modulus at relatively small particle concentrations. The tensile strength (Figure 8) is reduced via the incorporation of neat Tween. Consequently, the best strength results are reached at 0.5 vol % in case of RM300 and AluC and 1 vol % for Kronos 2310. Higher filler contents show an enhanced reduction in strength. Still, the reinforced PA6 (RM300) shows a little lower tensile strength compared with the neat PA6 (4%). The tensile strength can be increase by nanoparticles in case of strong nanoparticle–matrix–interaction[15,16] and a high dispersion quality[17] which is not sufficient in the present results. Tween alone increases the material properties, but nanoparticles improve Young's modulus and elongation at break even more.

Figure 9 represents the sum up of mechanical properties—e.g., Charpy notched impact toughness—of the material compositions. PA6-nanocomposites with excellent mechanical properties (stiffness/toughness) could be realized with the incorporation of Tween stabilized nanoparticle dispersions. Especially the elongation at break is increased three times using minimal amounts (0.56 vol %) TiO_2 (RM300) as particles. At the same time Charpy notched impact toughness could be increased about more than 20% and the Young's modulus more than 16% with just slightly reduced tensile strength (4%). Charpy impact toughness could be increased by incorporating neat Tween to the maximum of >20%, which is more than reached with incorporation of nanoparticles. But the nanoparticles have to be applied for an increase in Young's modulus and elongation at break resulting in a synergetic effect between Tween stabilized nanoparticles and PA6 matrix.

Comparison with Traditionally Compounded Nanocomposites (Kneader)

A conventional production method (measuring kneader) was performed in order to compare the resulting dispersion qualities with those gained via direct injection molding. Therefore, PA6 was molten in a kneader before nanoparticle containing dispersions (Tween as dispersing agent) were incorporated. The resulting filler contents are given in Table I. Evidently, in case of Al_2O_3 this method works better than IM due to the effect that the dispersion is directly injected in a closed mixing chamber, gaining a higher maximum volume content.

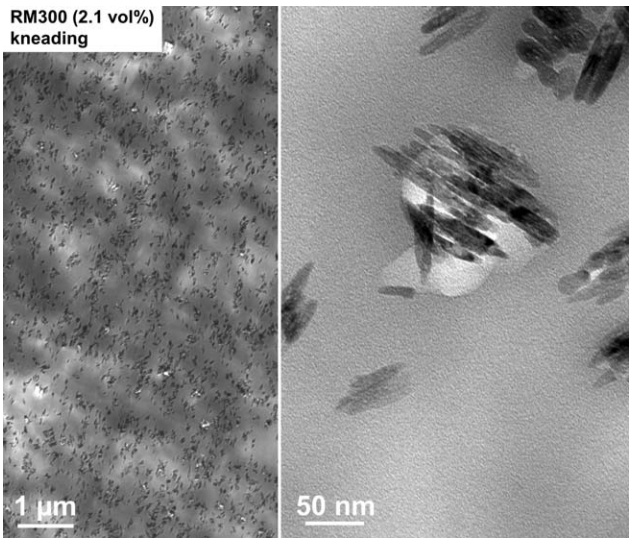

Figure 11. TEM image of RM300 TiO_2 nanoparticles incorporated in the PA6 matrix in a kneader.

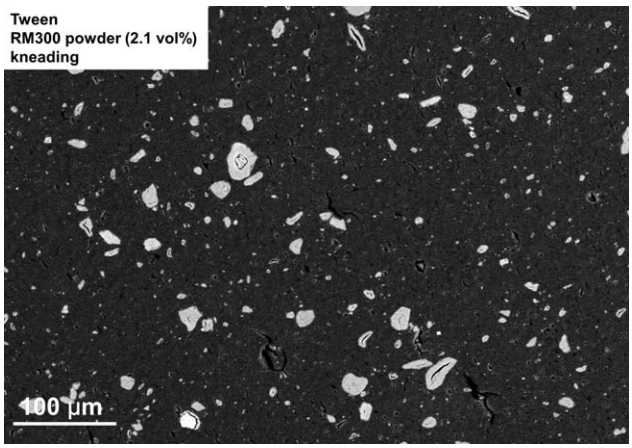

Figure 13. REM image of a PA6 mixed with Tween in a first step and then with RM300 nanoparticle powder in a second step.

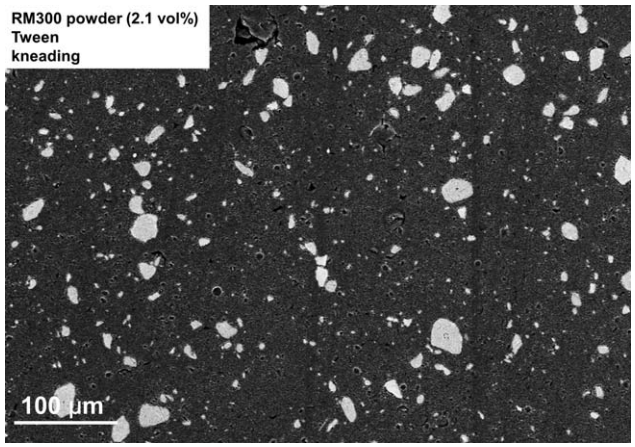

Figure 14. REM image of a PA6 mixed with RM300 nanoparticle powder in a first step and then with Tween in a second step.

Figure 10 presents the polished surface of PA6-Kronos TiO_2-particles compounds showing a very good dispersion achieved via kneader compared with the very good dispersion reached by the injection molding technique (Figure 1).

Figure 11 shows a very good dispersion and distribution quality of RM300 in PA6 using Tween as dispersing agent in a measuring kneader. The high magnification image (Figure 11 right) shows a very small agglomerate (50–100 nm) and the needle like shape of the RM300 TiO_2 nanoparticles is visual. Also bigger agglomerates of 200–700 nm can be found. These particles cannot be seen using an electron microscope (SEM) independent of the incorporation method which is an effect of the well embedded particles. It has been proved that particles seen in TEM but not evident in SEM are very well distributed, which can be achieved via kneader as well as injection molding techniques. Independent of the chosen processing method (kneader/IM) we are able to produce equal dispersion qualities. Thus, injection molding using Tween stabilized dispersions is a practicable method to produce nanocomposites in a single production step with promising mechanical properties. Using IM as well as kneading processes the quality of the applied nanoparticle containing dispersions is essential. In this case Tween is a proven ideal dispersing agent. The aim is to install melt processing methods for creating nanocomposites in such way, that the distribution processing is the main part of the process steps. The dispersing process takes place along the production of the nanoparticle containing dispersions. In the next step, these stabilized nanoparticles have to be distributed in the polymer melt.

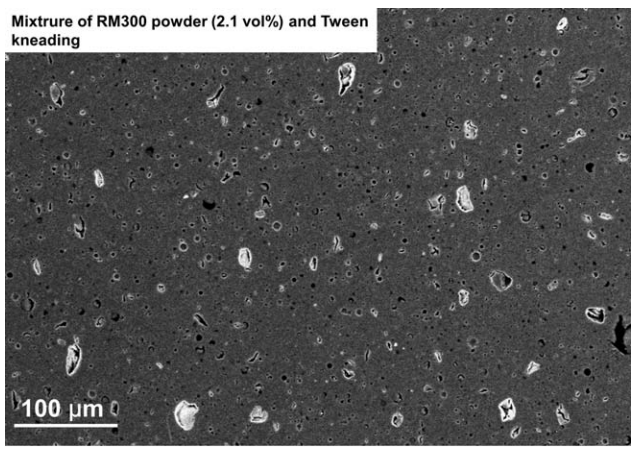

Figure 15. REM image of material consisting of PA6 and a pre mixture of RM300 TiO_2 nanoparticles and Tween mixed slightly by hand produced in a kneader.

As contrast Figures 12–14 give the SEM images of compounds that are produced by the incorporation of nanoparticles as powders. Tween is either not applied (Figure 12) or incorporated after or before nanoparticle powder insertion [Figure 13(a) and 14(a), respectively]. Finally, Figure 15 demonstrates the deagglomeration of a manually premixed Tween-TiO_2-Dispersion.

Figure 12 gives the SEM image of RM300 powder being incorporated via measuring kneader in the melted polymer. The nanoparticles are highly agglomerated in the powdery form and the agglomerates cannot be deagglomerated sufficiently in the kneading process. Literature has shown that nanoparticle powders deagglomerate insufficiently via extrusion processes.[3,8]

The effect of Tween is analyzed in Figures 13 and 14 where PA6 is melted in the kneader and first Tween is incorporated then the RM300 nanoparticle powder (Figure 13) or first the RM300 nanoparticle powder then the Tween is incorporated (Figure 14). Both images reveal a bad degree of deagglomeration reached with this method. Incorporating a slightly premixed RM300-Tween-dispersion leads to a bad degree of dispersion, as well (Figure 15). Tween and RM300 powder are manually mixed. Then this dispersion is incorporated in the melted polymer. Nevertheless, the resulting quality of nanoparticle dispersion in PA6 is better than from a separate incorporation. Thus, we need a very good dispersion quality in the starting nanoparticle-Tween 20 dispersion for reaching the very good dispersion quality in the nanocomposite. This can be gained by the incorporation of nanoparticle dispersions with Tween 20 as dispersing agent.

CONCLUSIONS

1. The direct insertion of Tween-stabilized nanoparticle dispersions in the injection molding processing results in a very good nanoparticle dispersion quality.
2. Nevertheless, the occurrence of individual primary particles is very rare.
3. The elongation at break could strongly be increased by incorporation of nanoparticles.
4. Elongation to break, Charpy notched impact toughness and *E*-modulus could be increased with slightly reduced tensile strength.
5. Incorporation of Tween-stabilized nanoparticle dispersion in a kneader yield in a comparably good dispersion quality as nanocomposites produced via direct injection molding.
6. Incorporating (a) nanoparticle powders, (b) nanoparticle powders and Tween separately, and (c) manually premixed nanoparticles with Tween does not lead to a sufficient dispersion quality of the nanoparticles in the polymer matrix.
7. A very good dispersion quality in the starting nanoparticle-Tween dispersion is needed for reaching a very good dispersion quality in the nanocomposite.

ACKNOWLEDGMENTS

The authors gratefully acknowledge the fundamental research grant "Artcom" funded by government Rheinland Pfalz.

REFERENCES

1. Knör, N.; Schröck, W.; Haupert, F.; Schlarb, A. K. 2nd Vienna International Conference, Micro- and Nano-Technology, **2007**, *2*, 283-288.
2. Wetzel, B. In IVW-Schriftenreihe; Schlarb, A. K., Ed.; Institut für Verbundwerkstoffe GmbH: Kaiserslautern, **2006**; Vol. *69*.
3. Thostenson, E.T.; Li, C.; Chou, T.W. *Compos. Sci. Technol.* **2005**, *65*, 491.
4. Ehrenstein, G. W. In Polymer Werkstoffe, 2nd ed., Hanser Publisher: Munich, Vienna, **1999**.
5. Karger-Kocsis, J.; Zhang, Z. In Mechanical Properties of Polymers Based on Nanostructures and Morphology; Balà-Calleja, J. F.; Michler, G., Eds.; Taylor and Francis Group: Boca Raton, London, New York, Singapore, **2005**; p 565.
6. Rauwendaal, C. In Polymer Extrusion; Hanser Publisher: Munich, Vienna, New York, **1990**.
7. Knör, N. F. In IVW-Schriftenreihe; Mitschang, P., Ed.; Institut für Verbundwerkstoffe GmbH: Kaiserslautern, **2010**; Vol. *93*.
8. Hassinger, I.; Burkhart, T. *J. Thermoplast. Compos. Mater.* **2011**, *25*, 573.
9. Bacher, A.; Berkei, M.; Drude, H.; Fuchs, T.; Guschin, V.; Kreitmeier, M.; Lüssenheide, S.; Metzger, J.; Meyer, H.; Mikonsaari, I.; Potyra, E.; Scholz, W.; Stein, J.; Tecklenburg, J.; Zanki, A. In Fraunhofer Institut für Chemische Technologie ICT; Mikonsaari, I., Ed.; Fraunhofer Verlag: Stuttgart, **2011**.
10. Frache, A.; Monticelli, O.; Ceccia, S.; Brucellaria, A.; Casale, A. *Polym. Eng. Sci.* **2008**, *48*, 2372.
11. Bartczak, Z.; Argon, A. S.; Cohen, R. E.; Weinberg, M. *Polym. J.* **1999**, *40*, 2347.
12. Wu, S. *J. Appl. Polym. Sci.* **1988**, *35*, 549.
13. Zhou, R.-J.; Burkhart, T. *J. Thermoplast. Compos. Mater.* **2010**, *23*, 487.
14. Jordan, J.; Jacob, K. I.; Tannenbaum, R.; Sharaf, M. A.; Jasiuk, I. *Mater. Sci. Eng. A* **2005**, *393*, 1.
15. Rong, M. Z.; Zhanga, M. Q.; Zhenga, Y. X.; Zeng, H. M.; Walter, R.; Friedrich, K. *Polym. J.* **2001**, *42*, 167.
16. Lehmann, B.; Friedrich, K.; Wu, C. L.; Zhang, M. Q.; Rong, M. Z.; *J. Mater. Sci. Lett.* **2003**, *22*, 1027.
17. Thio, Y.; Argon, A; Cohen, R.; Weinberg, M. *Polym. J.* **2002**, *43*, 3661.